Applied Mechanics and Materials
ISSN: 1662-7482, Vols. 773-774, pp 642-646
doi:10.4028/www.scientific.net/AMM.773-774.642
© 2015 The Author(s). Published by Trans Tech Publications Ltd, Switzerland.
Submitted: 2014-08-06
Revised: 2014-11-24
Accepted: 2014-11-24
Online: 2015-07-15

The fabrication of PSi/ZnO nanostructures as chemical sensors for the detection of ethanol in solution using an electrochemical impedance technique

F.S. Husairi[1,2, a], K. Eswar[1,2], Z. N. Atikah[1,2], A. Azlinda[1,2], M. Rusop[1,3], S. Abdullah[1,2, b]

[1]NANO-SciTech Centre (NST), Institute of Science;
[2]Faculty of Applied Sciences;
[3]NANO-ElecTronic Centre (NET), Faculty of Electrical Engineering;
Universiti Teknologi MARA (UiTM),
40450 Shah Alam, Selangor, Malaysia
[a]mhusairifadzilah@yahoo.com, [b]saifolabdullah@yahoo.co.uk

Keyword: PSi/ZnO nanostructure chemical sensor, FESEM, photoluminescence spectrometry, ethanol

Abstract. In this work, porous silicon (PSi) was prepared by electrochemical etching and used as a template for ZnO nanostructures. ZnO nanostructures were grown using the catalytic immersion method at different molar ratio concentrations of the precursor and stabilizer. The ZnO nanostructures were analyzed using FESEM and photoluminescence (PL) spectrometry, before tested with ethanol solution. The population of the ZnO nanostructures on PSi increased with the concentration and followed the surface morphology of PSi. The photoluminescence spectra of ZnO show two dominant peaks in the UV and visible regions. When the concentration of the precursor increased, the PL peaks in the visible region (630 nm) shifted towards the blue region of the spectrum. The PSi/ZnO nanostructure chemical sensor has a large surface area, reversing sensor and fast response in ethanol. The performance of the sensor was affected by the morphology and defect structures of the ZnO nanostructures layer.

Introduction

In the semiconductor industry, many types of materials, such as silicon, gallium arsenic, titanium dioxide and zinc oxide (ZnO), are used as base materials. Among them, ZnO is a unique material that has a wide bandgap of 3.37eV and a large exciton energy of 60 meV.[1] ZnO nanostructures can be used in many application areas, such as optoelectronics,[2] sensors,[3] transducers and biomedical science. ZnO is a piezoelectric material that can be used in sensor and transducer applications. ZnO nanostructures grown on Si-based substrates receive significant attention silicon is stable and resistant to high temperatures. Porous silicon nanostructures (PSiNs) has a rough surface morphology, which is a good template for growing ZnO nanostructures without using metal catalysts [4] because a rough surface provides good sites for ZnO to grow with minimum stress applied between the ZnO and PSi layer [5, 6]. ZnO nanostructures have been synthesised by various methods, such as chemical vapour deposition, an electrochemical method, RF magnetron sputtering and the sol-gel method [7-10]. In this work the sol-gel thermal solution-immersion method was selected because of its simplicity, safety, low cost, low-temperature deposition and large coating area. The urea was used as a stabilizer and zinc nitrate hexahydrate as a precursor to synthesize the ZnO nanostructures on PSi at different concentrations without using any catalyst material. ZnO deposited on PSiNs formed a flower-like structure and honeycomb-like network structures. The as-grown ZnO nanostructures were characterized using FESEM and PL spectroscopy and then tested with ethanol solution by using EIS measurement.

This article is an open access article under the terms and conditions of the Creative Commons Attribution (CC BY) license (https://creativecommons.org/licenses/by/4.0)

Methodology

In this work, ZnO nanostructures were grown on PSi by the thermal immersion method using $Zn(NO_3)_26H_2O$ as a precursors and CH_4N_2O as a stabiliser [11]. PSi was prepared through electrochemical etching method [12]. For the solution preparation, the molar ratios of $Zn(NO_3)_26H_2O$ to CH_4N_2O in a total volume of 100 ml were 2:1, 1:1, 1:2, 1:4 and 1:6. The aqueous solution was stirred and heated at 60^{o}C for 1 hour and followed by a 24-hour ageing process to produce a homogenous solution. After the ageing process, the PSiNs were inserted into test tubes filled with 50 ml of the solutions with different molar ratio concentrations. The test tubes were immersed in a water bath at a temperature of 90^{o}C. After 4 hours, the samples were dried for 1 hour at a temperature 150^{o}C and were annealed at 500^{o}C for 1 hour. The ZnO nanostructures were characterized by field emission scanning electron microscopy (JSM-7600F) and photoluminescence (HORIBA JOBIN YVON, PL). The chemical testing was coming out using electrochemical impedance spectroscopy (EIS) with a frequency between 0.1 and 32 MHz.

Results and Discussion

The morphology of ZnO nanostructures grown on the PSi surface was shown in Figure 1. The PSi surface is a sponge-like structure, which consists of a large number of pores on the surface help the ZnO nanostructures to incorporate into the pores. Different precursor concentrations in the solution contribute to the different sizes and morphologies of the ZnO nanostructures. When ZnO is deposited on PSi, it is deposited along the outer wall of the pores of the PSiNs, either partially or completely covering the porous surface. The morphology of the ZnO deposited on the PSi at different precursor concentrations shows the ZnO honeycomb-like network, nanoflowers and porous-like structures indicated in Figs. 1(b), 1(c-d) and 1(e). A crack-like structures was formed in Fig. 1 (a) with no flower structures exited on the surface. As shown in Fig. 1(b-e), as-grown ZnO nanoflowers have a diameter approximately 1 μm at the observed area on the PSiNs. When the concentration of the precursor increases, the ZnO has grown on the PSi becomes denser. A honeycomb-like ZnO network structure is found in samples prepared in 1:1 because the ZnO had grown on the wall of the PSi and followed the orientation of the wall to form a large diameter pore. As we see in Fig. 1(d-e), the surface morphology of the PSi surface has pores that are filled with small particles with a uniform grain size.

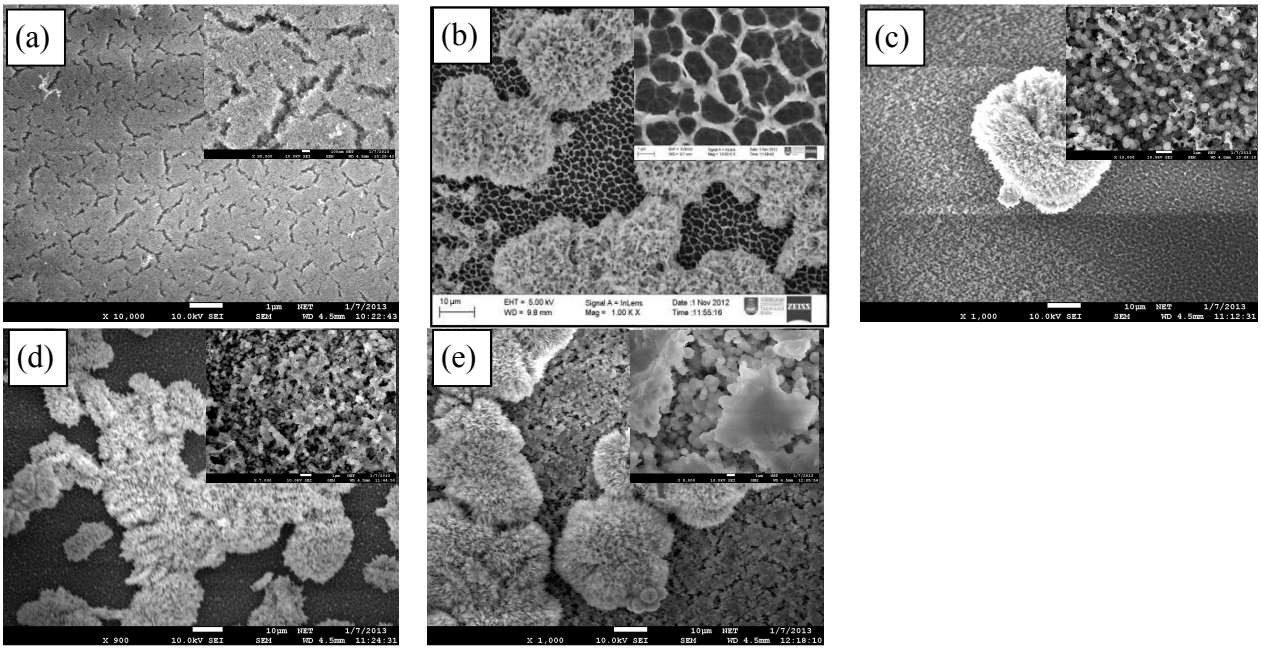

Fig 1. The FESEM image of ZnO nanostructures deposited of PSi at different molar ratios of $Zn(NO_3)_26H_2O$:CH_4N_2O, (a) 2:1, (b) 1:1, (c) 1:2, (d) 1:4 and (e) 1:6.

Figure 2 shows the PL spectrum of the ZnO nanostructures at varying stabilizer concentrations. Two emitting bands, including a UV emission at 385 – 415 nm and an orange band at 585 – 620 nm was observed. Peaks centered at the UV band-edge are attributed to near band gap emission (NBE) and the emissions in the visible range are due to the recombination of photogenerated holes with singly ionized charge states in intrinsic defects, such as oxygen vacancies and interstitial zinc [13, 14]. The ZnO has grown in the lowest concentration of stabilizer (CH_4N_2O) solution (0.1 M), has a weak violet emission. When the concentration of the stabilizer was increased, the intensity of the UV emission also increased. The crystallinity of the ZnO synthesised at a 1:6 is higher compare to the other samples because the intensity of the UV emission can be used to indicate the crystallinity of the ZnO nanostructures [13].

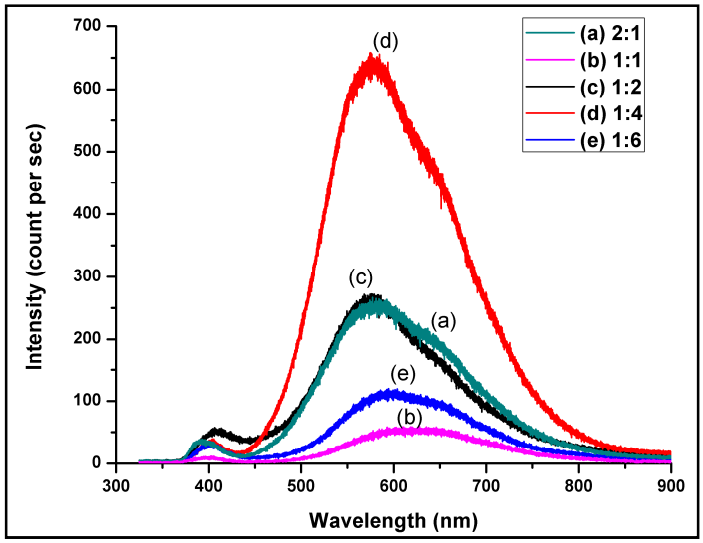

Fig 2. Photoluminescence spectra of the ZnO nanostructures produced at room temperature.

The emission near the yellow region is most likely cause by two factors. First, this emission can be caused by an excess of oxygen and the presence of hydroxyl (OH) groups, which were found in ZnO synthesised using the thermal immersion method [15, 16]. The formation of interstitial oxygen ions can be caused by aqueous chemical growth because this growth method is oxygen rich for ZnO [17].

3.5 PSi/ZnO nanostructures Chemical Sensor

The resistance of the PSi/ZnO nanostructures decreases with exposure time. The response can be calculated using the formula below:

$$Response\ (\%) = \frac{(R_o - R_s)}{R_0} \times 100\%$$

where R_o is a resistance before exposure and R_s is the resistance after exposure. Changing the parameters of the sample preparation will affect the morphological properties and the sensor characteristics [18]. The fast response of the PSi/ZnO sensor to ethanol solution might be due to the regular morphology and suitable thickness for sensing. The responses of the sensors are shown in figure 3. PSi/ZnO nanostructures prepared at ratio 2:1 and 1:4 show the best response with fast and consistent response to ethanol solution. The change in resistance value in 2 minutes was 87% and 89% respectively. The response, increased by time with the maximum value approach at 98% for 1:4. The response for 2:1 take a longer time compare with 1:4 to approach maximum response. The lowest sensor response recorded at sample ratio 1:1 with maximum response at 4 minutes first and goes down after 10 minutes.

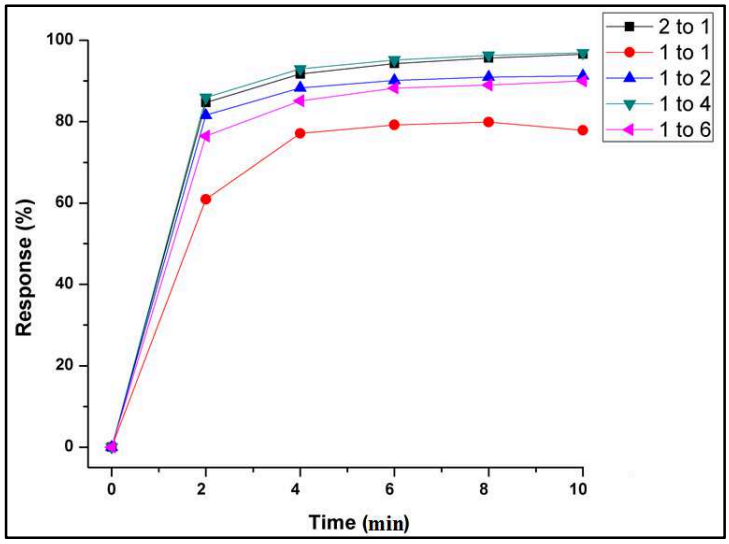

Fig 3. The response of the ZnO nanostructures versus time after exposing to the ethanol solution.

The response of PSi/ZnO nanostructures sensor was depended mainly on the ZnO nanostructures deposited. The sample prepared in 1:6 molar of $Zn(NO_3)_26H_2O$:CH_4N_2O had a lower defect structure and small area of active sites for sensing. This morphology makes the reaction between the ethanol solution and oxygen species in the ZnO layer smaller when compared to the other samples. The PSi also gives the minimum effect to this sample. The sample prepared in 1:4 shows a higher sensitivity than the other samples as observed in the 85.96% response when exposed to ethanol for 2 minutes. The response was increased in small value from 2 to 10 minutes. Based on the photoluminescence result of the corresponding peak in the visible region, samples 1:4 possess a high concentration of oxygen defects in the form of interstitial oxygen and deep-level defects introduced in the film. The effect of PSiNs gives the additional advantage of this sample to sense the ethanol solution in maximum response. So, it can be concluded that, PSi/ZnO nanostructures prepared in 1:4 molar of $Zn(NO_3)_26H_2O$:CH_4N_2O solution as an optimized sample in term of sensor response.

Conclusion

We have presented ZnO nanostructure chemical sensors synthesized by using a thermal immersion method to detect ethanol solution. The surface morphology made the sensor is efficient at absorbing and desorbing ethanol molecules. Furthermore, based on our results and analysis, a higher sensitivity, faster response/recovery could be obtained using PSi/ZnO nanostructures prepared at ratio 1:4 of $Zn(NO_3)_26H_2O$:CH_4N_2O solution. The detection and identification of ethanol could be improved by using the appropriate structures and operation parameters for the PSi/ZnO nanostructure chemical sensors.

References

[1] R. C. Pawar, J. S. Shaikh, A. A. Babar, P. M. Dhere, and P. S. Patil, "Aqueous chemical growth of ZnO disks, rods, spindles and flowers: pH dependency and photoelectrochemical properties," *Solar Energy,* vol. 85, pp. 1119-1127, 2011.

[2] Z. Z. Ye, J. G. Lu, Y. Z. Zhang, Y. J. Zeng, L. L. Chen, F. Zhuge, G. D. Yuan, H. P. He, L. P. Zhu, J. Y. Huang, and B. H. Zhao, "ZnO light-emitting diodes fabricated on Si substrates with homobuffer layers," *Applied Physics Letters,* vol. 91, pp. 503-505, 2007.

[3] Y. Cao, P. Hu, W. Pan, Y. Huang, and D. Jia, "Methanal and xylene sensors based on ZnO nanoparticles and nanorods prepared by room-temperature solid-state chemical reaction," *Sensors and Actuators B: Chemical,* vol. 134, pp. 462-466, 2008.

[4] H.-C. Hsu, C.-S. Cheng, C.-C. Chang, S. Yang, C.-S. Chang, and W.-F. Hsieh, "Orientation-enhanced growth and optical properties of ZnO nanowires grown on porous silicon substrates," *Nanotechnology,* vol. 16, pp. 297–301, 2005.

[5] J. W. Jie, G. Wang, Q. Chen, Y. Han, X. Wang, X. Hou, J. G, "Synthesis and Characterization of Aligned ZnO Nanorods on Porous Aluminum Oxide Template," *Journal of Physical Chemistry B,* vol. 108, pp. 11976-11980, 2004.

[6] Z. L. Wang, "Novel nanostructures of ZnO for nanoscale photonics, optoelectronics, piezoelectricity, and sensing," *Applied Physics A: Materials Science & Processing,* vol. 88, pp. 7-15, 2007.

[7] J. W. Zhao, L. R. Qin, Z. D. Xiao, and L. D. Zhang, "Synthesis and characterization of novel flower-shaped ZnO nanostructures," *Materials Chemistry and Physics,* vol. 105, pp. 194-198, 2007.

[8] H. Kou, X. Zhang, Y. Du, W. Ye, S. Lin, and C. Wang, "Electrochemical synthesis of ZnO nanoflowers and nanosheets on porous Si as photoelectric materials," *Applied Surface Science,* vol. 257, pp. 4643-4649, 2011.

[9] H. Cai, H. Shen, Y. Yin, L. Lu, J. Shen, and Z. Tang, "The effects of porous silicon on the crystalline properties of ZnO thin films," *Journal of Physics and Chemistry of Solids,* vol. 70, pp. 967-971, 2009.

[10] S. Amizam, H. A. Rafaie, M. H. Mamat, Z. Khusaimi, M. Z. Sahdan, S. Abdullah, and M. Rusop, "Study On Structural And Optical Properties On The Effect of Deposition Time on The ZnO Nanorods Grown On Porous Silicon Substrate," *Solid State Science and Technology,* vol. 18, pp. 343-348, 2010.

[11] F. S. Husairi, S. A. M. Zobir, M. Rusop, and S. Abdullah, "Electrical properties of carbon nanotubes synthesis by double furnace thermal-CVD technique at different temperatures on porous silicon template," *IOP Conference Series: Materials Science and Engineering,* vol. 46, p. 012023, 2013.

[12] F. S. Husairi, J. Rouhi, K. A. Eswar, A. Z. Zainurul, M. Rusop, and S. Abdullah, "Electrochemical impedance spectroscopy analysis of porous silicon prepared by photo-electrochemical etching: current density effect," *Applied Physics A,* pp. 1-6, 2014/05/01 2014.

[13] E. Bacaksiz, S. Yılmaz, M. Parlak, A. Varilci, and M. Altunbaş, "Effects of annealing temperature on the structural and optical properties of ZnO hexagonal pyramids," *Journal of Alloys and Compounds,* vol. 478, pp. 367-370, 2009.

[14] G. Kenanakis, M. Androulidaki, E. Koudoumas, C. Savvakis, and N. Katsarakis, "Photoluminescence of ZnO nanostructures grown by the aqueous chemical growth technique," *Superlattices and Microstructures,* vol. 42, pp. 473-478, 2007.

[15] S. A. Kamaruddin, K. Y. Chan, M. Z. Sahdan, M. Rusop, and H. Saim, "ZnO microstructures and nanostructures prepared by sol-gel hydrothermal technique," *Journal Nanoscience Nanotechnology,* vol. 10, pp. 5618-22, 2010.

[16] Z. Khusaimi, S. Amizam, M. H. Mamat, M. Z. Sahdan, M. K. Ahmad, N. Abdullah, and M. Rusop, "Controlled Growth of Zinc Oxide Nanorods by Aqueous-Solution Method," *Synthesis and Reactivity in Inorganic, Metal-Organic, and Nano-Metal Chemistry,* vol. 40, pp. 190-194, 2010.

[17] S. N. Bai, H. H. Tsai, and T. Y. Tseng, "Structural and optical properties of Al-doped ZnO nanowires synthesized by hydrothermal method," *Thin Solid Films,* vol. 516, pp. 155-158, 2007.

[18] D. G. Yarkin, "Impedance of humidity sensitive metal/porous silicon/n-Si structures," *Sensors and Actuators A Physical,* vol. 107, pp. 1-6, 2003.